A structural study of seven *N*-acylindolines and their Pd(II)-mediated intramolecular oxidative coupling reactions for the synthesis of pyrrolophenanthridone alkaloids

Ruth Feilcke[a], Richard Goddard[b], Peter Imming[a*], Rüdiger W. Seidel[a*]

[a] Institut für Pharmazie, Martin-Luther-Universität Halle-Wittenberg, Wolfgang-Langenbeck-Straße 4, 06120 Halle (Saale), Germany

[b] Max-Planck-Institut für Kohlenforschung, Kaiser-Wilhelm-Platz 1, 45470 Mülheim an der Ruhr, Germany

[*] Corresponding authors

E-Mail: peter.imming@pharmazie.uni-halle.de, ruediger.seidel@pharmazie.uni-halle.de

Phone: 49 345 5525175

Fax: 49 345 5527027

Abstract

Direct synthesis of the pyrrolophenanthridone scaffold was explored using an intramolecular Pd(II)-mediated coupling reaction of different *N*-acylindolines *via* C–H activation, *Amaryllidaceae* alkaloids of the lycorine type belong to this type. Depending on the substitution pattern of the starting materials, the pathway yielded different product patterns and yields. Introduction of electron-withdrawing substituents into the 6-position of the indoline moiety did not improve coupling. Seven *N*-acylindoline precursors were structurally characterized by X-ray crystallography and NMR spectroscopy. The crystal structure of the lycorine type alkaloid oxoassoanine is reported for the first time.

Keywords: Oxoassoanine; *N*-Acylindoline; Phenanthridone; Palladium; Crystal structure

1. Introduction

Amaryllidaceae alkaloids are a diverse group of natural products isolated from one of the approximately 2260 species of 80 genera that belong to the *Amaryllidaceae* family [1]. They are classified in nine structural types based on their biosynthetic pathway [2]. One of these is the lycorine type, which possesses a pyrrolophenanthridone skeleton (Scheme 1) with a dioxol or a similar functional group. One important example is oxoassoanine, which was originally isolated from aerial parts of *Narcissus assoanus* Duf. in 1986 [3]. It is the precursor of pratosine, which was identified in 1983 as constituent of bulbs of *Crinum latifolium* L. [4].

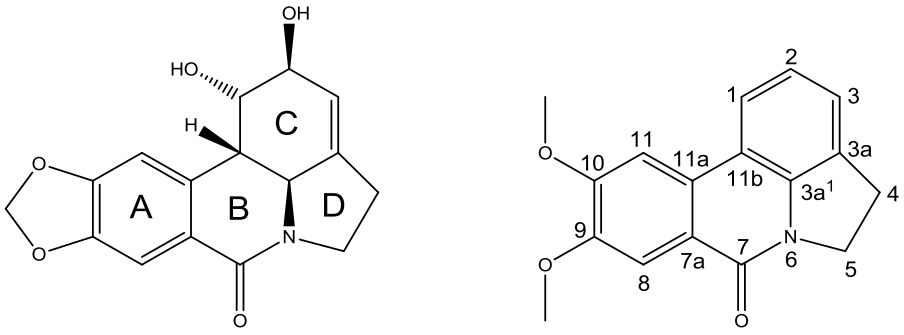

Scheme 1. Chemical diagrams of the *Amaryllidaceae* alkaloids lycorine and oxoassoanine, showing the conventional ring labelling and atom numbering of the pyrrolophenanthridone skeleton.

Crinum is the largest genus within *Amaryllidaceae* and *Crinum* species have been widely used in traditional medicine to treat different kinds of ailments [5]. Alkaloids of the lycorine type exhibit a variety of pharmacological properties, *e.g.* anti-cancer [6-9], anti-bacterial [10, 11], anti-fungal [10, 11] and anti-viral [12, 13], and are therefore of particular interest in drug discovery.

A straightforward synthesis of the pyrrolophenanthridone scaffold using an intramolecular Pd(II)-mediated coupling reaction of *N*-acylindolines *via* C–H activation was first reported by Black *et al.* [14, 15]. It is thus of interest to investigate the Pd(II)-mediated oxidative coupling of a variety of *N*-acylindolines to determine scope and limitations of this reaction in the preparation of compounds with the pyrrolophenanthridone scaffold. Of particular importance is how the structure of the *N*-acylindoline precursors affects the resulting products. Herein, we describe the preparation and structural characterization of a variety of *N*-acylindoline precursors and the identification of the products of the Pd(II)-

mediated oxidative coupling reactions, including the first crystal structure analysis of the alkaloid oxoassoanine.

2. Results and discussion

2.1. Synthesis and structural elucidation of *N*-acylindolines 1a-1g

N-acylindolines **1a-1g** (Scheme 2) were readily obtained in satisfactory yields by condensation of the respective acid chloride with indoline and 6-substituted indolines in the presence of a base [16]. The acid chlorides were either purchased or prepared from the corresponding free carboxylic acid by treatment with thionyl chloride and reacted *in situ* with the indoline component. The structures of **1a-1g** were confirmed by NMR and high resolution mass spectrometry. The syntheses of compounds **1a** [17-19], **1b** [16, 20, 21] and **1c** [17-19] *via* different routes were previously reported in the literature. Compounds **1a-g** were characterized by single-crystal X-ray analysis in this work. With the exception of **1a**, the *N*-acylindolines studied were encountered exclusively in a (*Z*)-conformation about the amide bond in the crystal, as depicted in Scheme 2. Owing to the twist of the phenyl ring out of the plane of the amide group, the molecules exhibit axial chirality about the C_{phenyl}–C_{amide} bond.

Compound **1a** crystallizes with two crystallographically unique molecules (*Z*' = 2). As shown in Figure 1, the two crystallographically distinct molecules differ not only in their conformation about the amide bond but also in the orientation of the piperonoyl moiety about the C_{phenyl}–C_{amide} bond with respect to the amide group. In the latter case, the corresponding difference is approximately 193° with respect to the N1–C8–C9–C10 torsion angle (Table 1). As expected, the amide moieties are nearly planar in both molecules. The distortion in an amide unit can most conveniently be expressed quantitatively by the Winkler-Dunitz parameters τ, χ(C) and χ(N), whereby τ describes the magnitude of rotation about the C(=O)–N bond and χ(C) and χ(N) the pyramidalities at the respective C and N atoms [22]. While a discussion of χ(C) can be reasonably neglected here, τ and χ(N) parameters are listed in Table 1. Comparison of χ(N) parameters reveals that the magnitude of pyramidality at the N atom in the amide moiety is similar in the (*Z*)- and (*E*)-conformers in the crystal structure of **1a**.

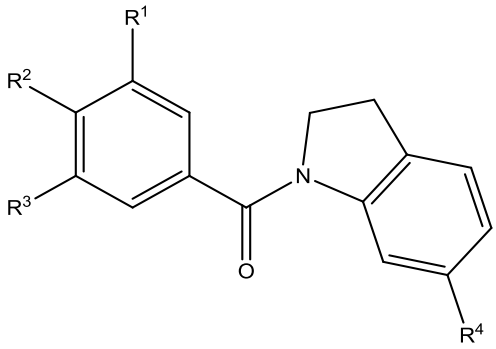

1a: R^1 = H, R^2 = R^3 = O-CH_2-O, R^4 = H
1b: R^1 = H, R^2 = OMe, R^3 = H, R^4 = H
1c: R^1 = H, R^2 = OMe, R^3 = OMe, R^4 = H
1d: R^1 = OMe, R^2 = OMe, R^3 = OMe, R^4 = H
1e: R^1 = H, R^2 = OBn, R^3 = OMe, R^4 = H
1f: R^1 = H, R^2 = OMe, R^3 = OMe, R^4 = NO_2
1g: R^1 = H, R^2 = OMe, R^3 = OMe, R^4 = CF_3

Scheme 2. Chemical diagram of *N*-acylindolines **1** studied in the present work. Here shown in the (*Z*)-conformation.

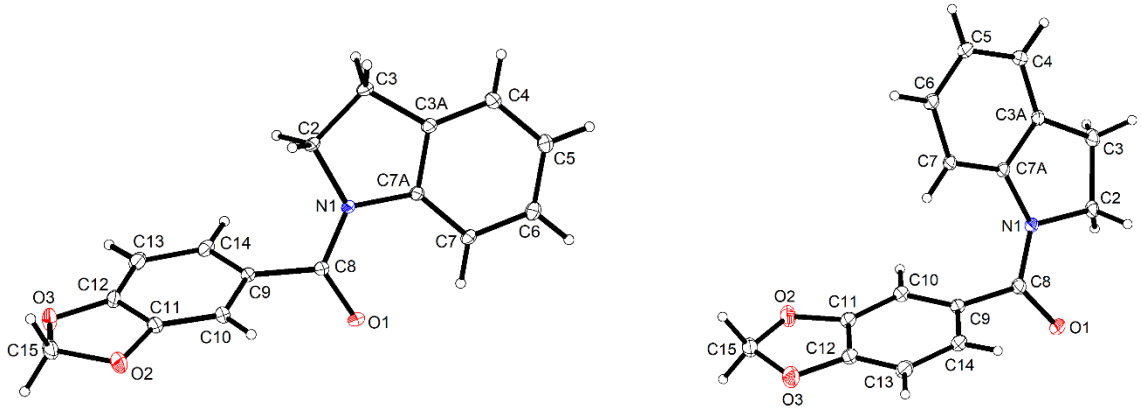

(a) **(b)**

Figure 1. Molecular structures of the two crystallographically distinct molecules in the crystal structure of **1a**, with (a) a (*Z*)-conformation and (b) an (*E*)-conformation about the amide bond. Displacement ellipsoids are drawn at the 50 % probability level. H atoms are represented by small spheres of arbitary radii.

Table 1. Selected geometric parameters for **1a-g**. The Winkler-Dunitz parameters [22] τ and χ(N) represent the twist angle about the amide linkage and pyramidality at the amide N atom, respectively (see text).

		O1–C8–N1–C7A	**N1–C8–C9–C10 / °**	**τ / °**	**χ(N) / °**
1a	(*Z*)-conformer	0.6(3)	–131.03(15)	–170.9	15.8
	(*E*)-conformer	–164.23(16)	62.1(2)	9.6	–13.5
1b		0.0(8)	–146.5(5)	–166.8	22.9
1c		–6.0(4)	54.4(4)	183.6	20.1
1d		–4.3(2)	–130.82(13)	182.9	16.3
1e		5.06(14)	–135.22(9)	–171.2	6.4
1f		0.1(5)	–143.3(3)	189.7	19.9
1g		–1.0(3)	51.0(3)	185.5	13.2

In contrast to **1a**, the crystal structures of **1b-g** contain only one crystallographically unique molecule, each adopting the (*Z*)-conformation about the amide bond. The molecular structures of **1b-g** in the crystal are depicted in Figure 2 and selected geometrical parameters are listed in Table 1. The methoxy groups of the *p*-anisoyl moiety **1b** and the veratroyl moieties in **1c**, **1f** and **1g** are virtually coplanar with the benzene rings. In the veratroyl moieties, the *ortho*-dimethoxybenzene group adopts a planar conformation with local C_{2v} symmetry, which probably represents the minimum energy conformation [23]. Likewise, the arrangement of the methoxy groups of the 3,4,5-trimethyoxybenzoyl moiety in **1d**, *i.e.* the two outer methoxy groups being coplanar with the benzene ring and the inner one perpendicular, as shown in Figure 2, corresponds to the preferred conformation of 1,2,3-trimethoxybenzene [24]. Similar to the piperonoyl moiety in the crystallographically distinct molecules in the crystal structure of **1a**, the orientation of the veratroyl moiety about C_{phenyl}–C_{amide} bond in **1f** differs from that in **1c** and **1g** approximately by a twofold rotation, as indicated by the N1–C8–C9–C10 torsion angles listed in Table 1. The largest magnitude of deviation from planarity of the amide linkage and the largest pyramidality at amide N atom is observed for **1b** in the crystal, as revealed by the τ and χ(N) parameters (Table 1), respectively. In general, mainly steric repulsion among the substituents at the amide group causes twist around the amide bond and pyramidalization at the N atom. The magnitude of deformation depends on the steric demand and electronic effects of the substituents. Considering that **1b** is the least sterically crowded one among the *N*-acylindolines studied, it can be assumed that the extent of

the deformation of the amide group observed in the solid-state is mainly governed by effects of crystal packing.

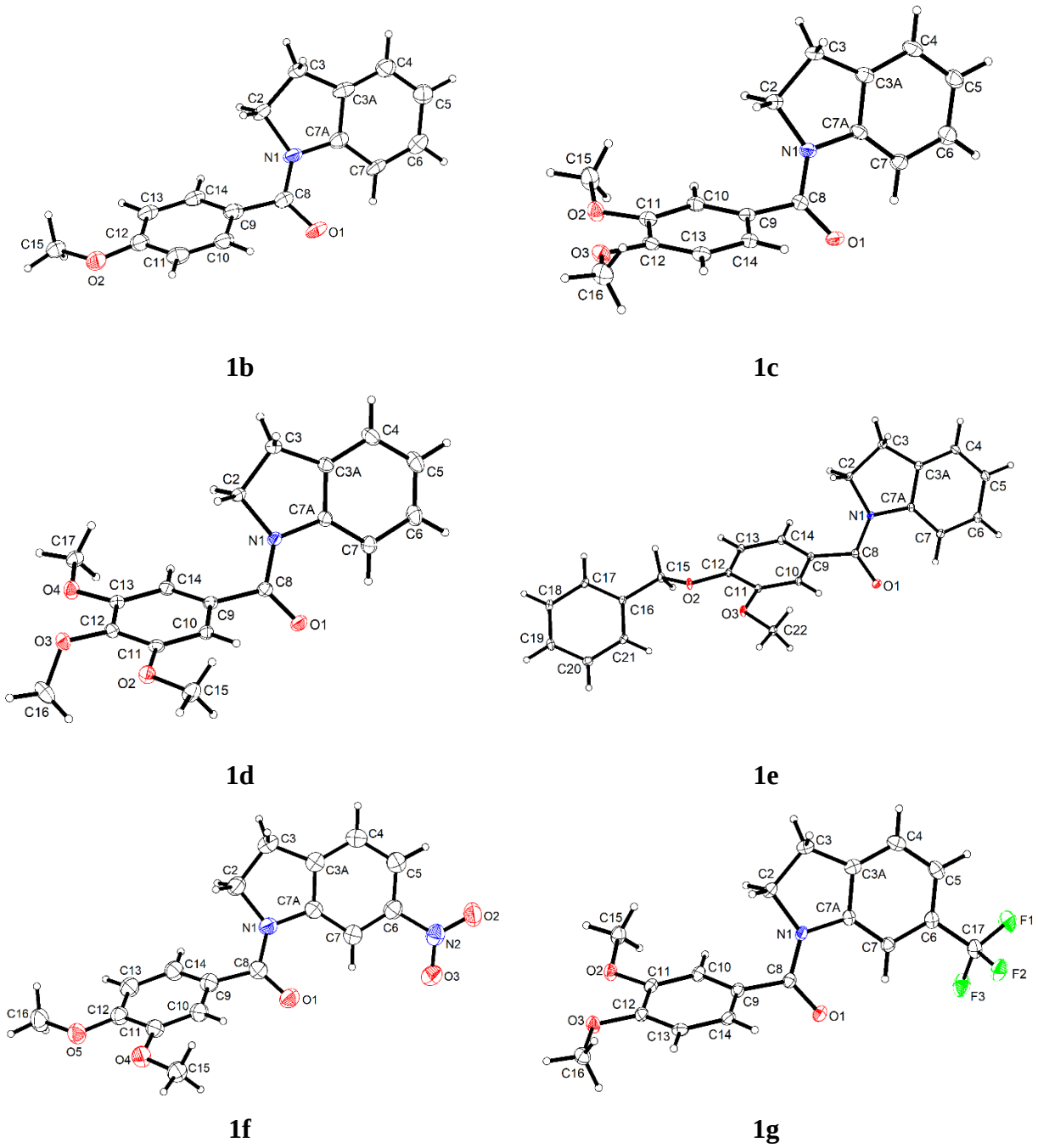

Figure 2. Molecular structures of **1b-g** in the crystals. Displacement ellipsoids are drawn at the 50 % probability level. H atoms are represented by small spheres of arbitray radii.

Since racemic mixtures tend to form centrosymmetric crystal structures [25], it is interesting to note that the crystal structure of **1b** is chiral (Sohnke space group), *i.e.* comprises only one conformational enantiomer of the axially chiral molecule, and the crystal structures of **1c** and **1f** are polar. In contrast, the crystal structures of **1a**, **1d, 1e** and **1g** are centrosymmetric racemates. It is worth noting that in spite of the different crystal environments, all molecules adopt a similar core conformation (Figure 3).

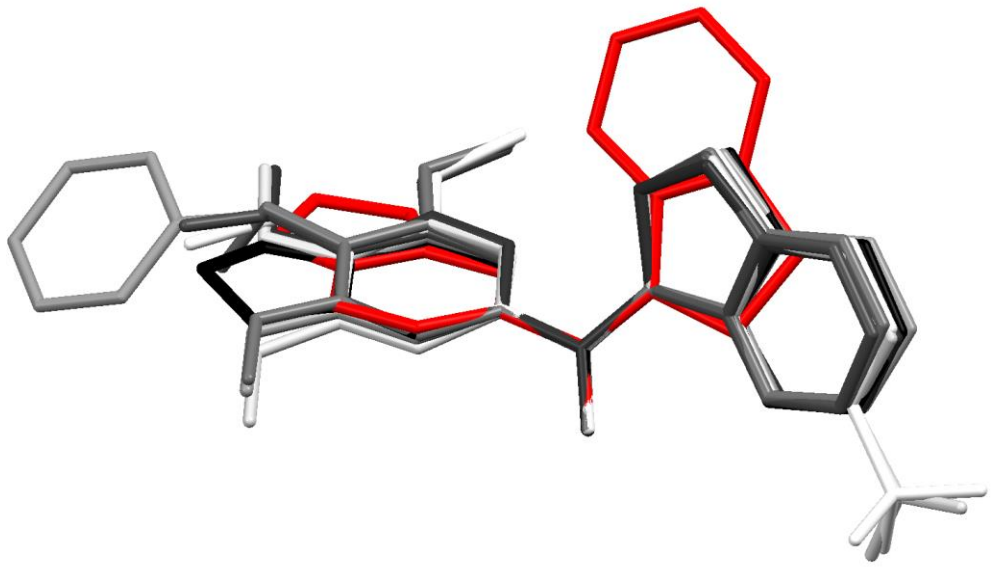

Figure 3. Superposition of the amide groups of **1a-g**, showing the similar conformations of the molecules in the solid state. Colour scheme: (*Z*)-**1a** black and (*E*)-**1a** red, **1b-g** various shades of grey from anthracite to white. H atoms are omitted for clarity.

Whereas the solid-state structures of the *N*-acylindolines **1b-g** are determined by close packing, a geometrical analysis of the crystal structure of **1a** revealed intermolecular interactions of the C–H···O and C–H···π type formed by the methylene acetal and the amide oxygen atom or the six-membered aromatic ring of the indoline moiety (Figure 4), which can be interpreted as weak hydrogen bonds. These contacts occur between the crystallographically distinct (*E*)- and (*Z*)-conformers of **1a** and, thus, may be considered a possible cause for the crystallization of this compound with Z' = 2. Due to the electron withdrawing effect of the acetal oxygen atoms, the acetal methylene group is prone to form weak hydrogen bonds. The polarity of this group is also reflected in a downfield shift of the corresponding signal in the ^{1}H NMR spectrum (δ_H = 6.043 ppm).

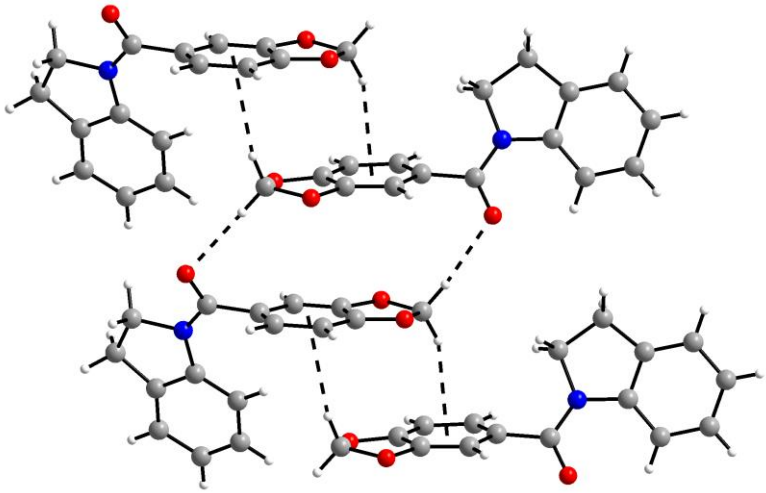

Figure 4. Association of (*E*)- and (*Z*)-conformers *via* weak hydrogen bonds (dashed lines) of the C–H···O [*D*···*A* = 3.29 and 3.32 Å] and C–H···π type [*D*···*Cg* = 3.62 and 3.76 Å] in the crystal structure of **1a**.

Kumar *et al.* pointed out that the ^{1}H NMR spectra of **1a** and **1c** show some unusual features, *viz.* only six signals in the aromatic region were observed at room temperature in $CDCl_3$, although seven were expected [19]. This observation is consistent with the spectral data reported previously by Ganton and Kerr [18]. The former authors, however, reported that in benzene-*d*6 in each case a broad downfield shifted signal appeared at ca. 8.1 ppm, which significantly sharpened upon heating the solution to 70 °C. Moreover, the same authors reported that in the case of **1c** in benzene-*d*6 four distinct ^{1}H NMR signals were observed for the two methoxy groups at room temperature, which coalesced while heating the sample to 70 °C. Kumar *et al.* ascribed these observations to restricted rotation about the amide linkage [19]. We can confirm the apparently missing signal in the aromatic region of the ^{1}H NMR spectra of these compounds at room temperature in $CDCl_3$, but we found no evidence for two distinct sets of the methoxy ^{1}H NMR signals when we re-recorded the ^{1}H NMR spectrum of **1c** in benzene-*d*6 (Figure 5). Therefore, it must be assumed that the rotation about the amide linkage and also the rotation about C_{phenyl}–C_{amide} bond in **1c** are actually fast on the NMR time scale under these conditions.

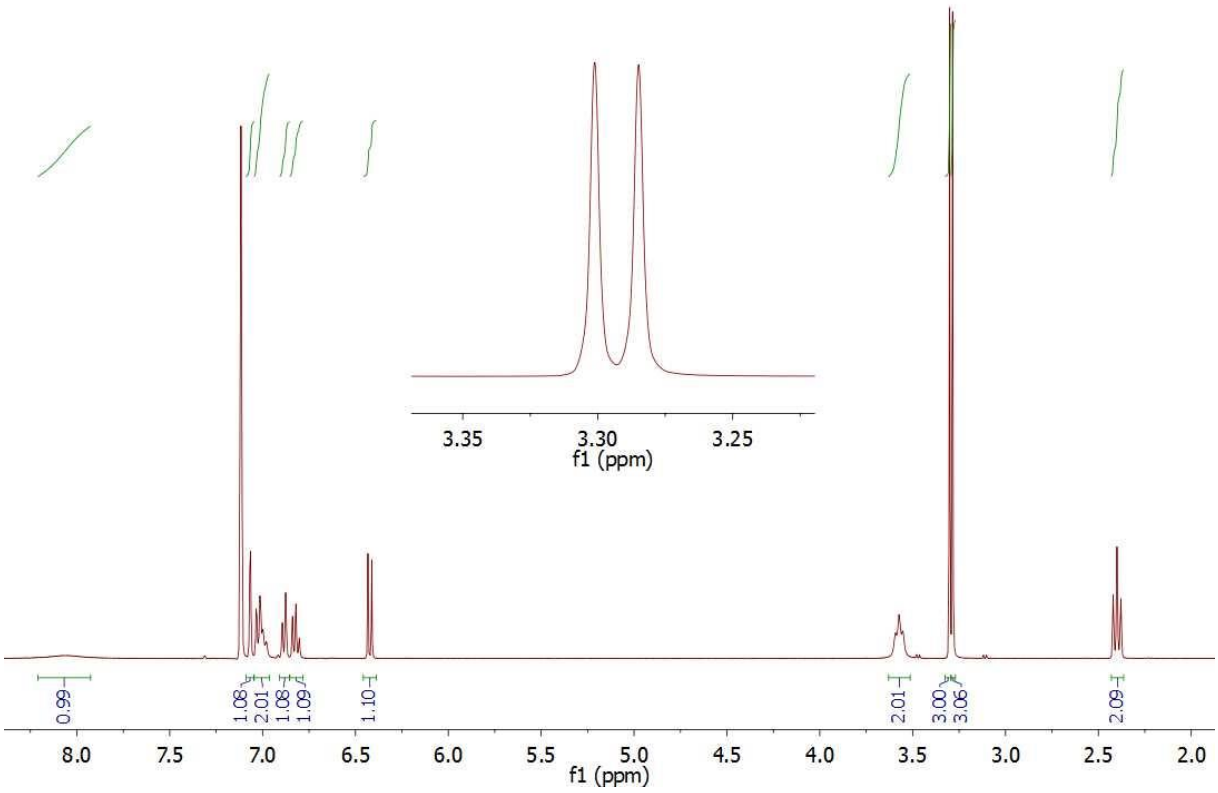

Figure 5. ^{1}H NMR spectrum of **1c** in benzene-*d*6 at room temperature.

The existence of both an (*E*)- and a (*Z*)-conformer in the crystal structure of **1a** prompted us to subject this compound to variable-temperature ^{1}H NMR measurements below room temperature to gain knowledge about restricted rotation. Figure 6 shows temperature-dependent ^{1}H NMR spectra of **1a** in $CDCl_3$. In the aliphatic region, the signal assigned to the 2-methylene position of the indoline group most markedly reveals a split into discrete sets of signals at low temperature. Coalescence is observed at approximately –10 °C. This can be attributed to restricted rotation about the amide linkage. In the aromatic region, two additional signals emerge upon lowering the temperature below –10 °C. At –50 °C, these doublets assigned to H7 of the indoline moiety are observed 8.06 and 6.08 ppm. Based on the observed shifts and comparison with (*Z*)-*N*-acetylindoline (δ_{H7} = 8.22 ppm in $CDCl_3$) and unsubstituted indoline (δ_{H7} = 6.45 ppm in $CDCl_3$) [26], the signals are tentatively assigned to the (*Z*)- and (*E*)-conformer, respectively. In the (*Z*)-conformer, the indoline H7 is in the proximity of the amide oxygen atom (H7···O1: ca. 2.32 Å in the crystal structure of **1a**). Most likely a field effect of the carbonyl group [26, 27] is responsible for the considerable downfield shift observed for the signal assigned to H7 in the (*Z*)-conformer. Above –10 °C, the signal assigned to H7 becomes virtually non-observable owing to extreme broadening. The

conformational analysis is reflected by the product pattern observed during coupling as will be described in the next paragraph.

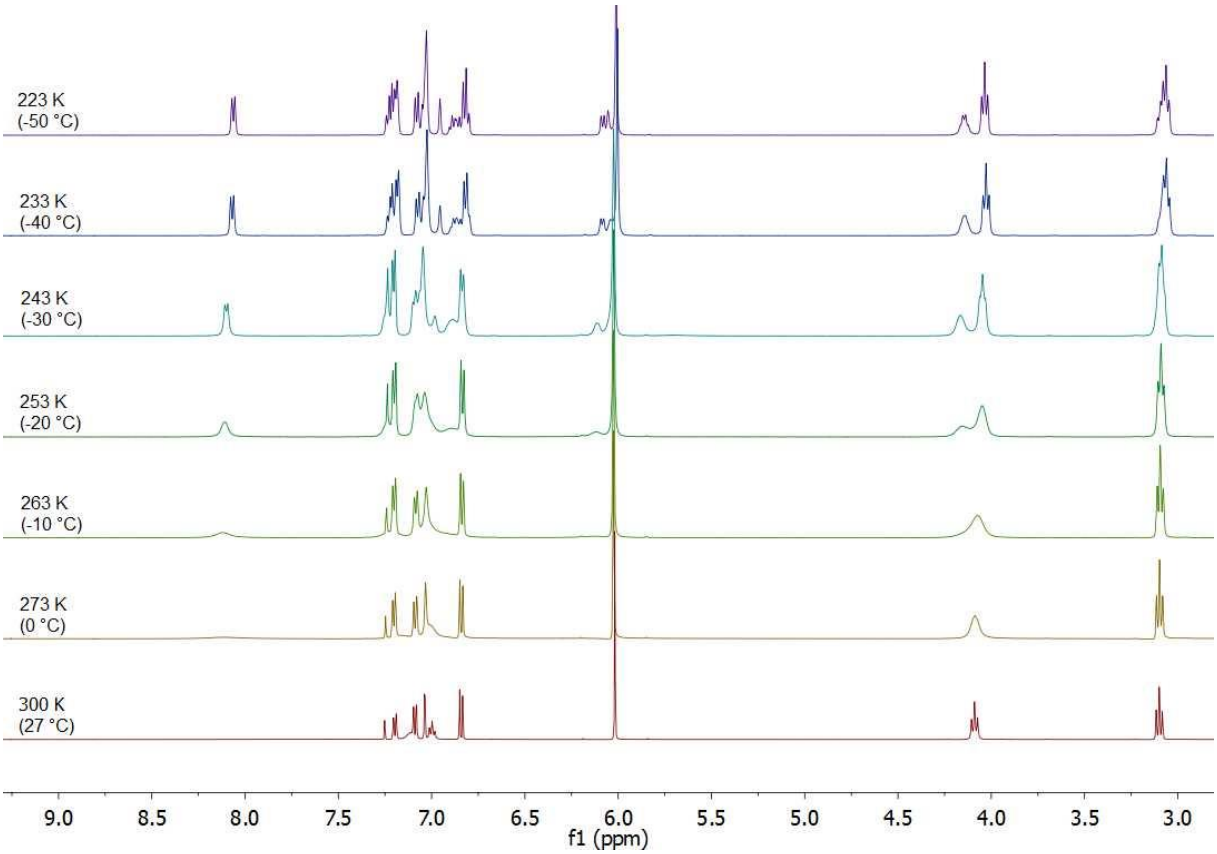

Figure 6. Temperature-dependent ^{1}H NMR spectra of **1a** in chloroform-*d*.

2.2. Intramolecular oxidative coupling reactions of 1a-g

The intramolecular oxidative biphenyl coupling of **1a-g** was studied using reaction conditions described by Black *et al.* [14], *i.e.* heating to reflux for five hours with one equivalent of $Pd(OAc)_2$ in glacial acetic acid (Scheme 3). If this worked, it would be the simplest and most straightforward pathway to this alkaloid class. Depending on the substitution pattern of the respective *N*-acylindoline **1**, we identified four types of products (**2**-**5**) under these conditions (Scheme 3). Moreover, oxidized starting material, *i.e.* the corresponding *N*-acylindole, and unreacted starting material (SM) were identified.

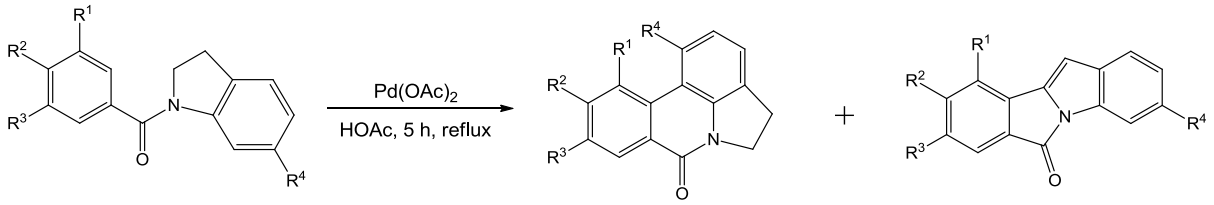

1

2a: R^1 = H, R^2 = R^3 = O-CH_2-O, R^4 = H
2b: R^1 = H, R^2 = OMe, R^3 = H, R^4 = H
2c: R^1 = H, R^2 = OMe, R^3 = OMe, R^4 = H
3a: R^1 = R^2 = O-CH_2-O, R^3 = H, R^4 = H

4a: R^1 = H, R^2 = R^3 = O-CH_2-O, R^4 = H
4c: R^1 = H, R^2 = OMe, R^3 = OMe, R^4 = H
5a: R^1 = R^2 = O-CH_2-O, R^3 = H, R^4 = H

Scheme 3. Reaction scheme and chemical diagrams of identified products **2-5**.

2a and **3a** were reported previously in the literature as products of intramolecular biphenyl coupling of **1a** [14] or iodinated **1a** [17]. Our attempts to separate the two regioisomers by fractional crystallization or column chromatography were unsuccessful. Harayama *et al.* reported successful separation of the two regioisomers by preparative thin-layer chromatography (TLC) [17], whereas Black *et al.* did not mention separation problems for **2a** and **3a** nor did they report NMR data for the compounds studied [14]. We additionally observed the formation of **4a** and **4c** during the reaction. Kirst reported the formation of **4** from iodinated and brominated *N*-benzyl indoline derivatives by hydrodehalogenation and aromatization as the sole product of a Pd(II)-mediated biphenyl coupling process instead of an intramolecular coupling [28]. For **1f**, we did not observe oxidation in contrast to **1a-1e** and **1g**. If the substitution pattern allowed intramolecular coupling, **4** and/or **5** could be identified in the reaction mixtures, since C2 is the most activated position in indoles [29]. In all cases, we recovered unreacted starting material, ranging from 18 % in the case of **1a** to 91 % in the case of **1d** (identified by TLC).

The literature regarding an understanding of the regioselectivity in coupling reactions through C–H activation is somewhat contradictory. According to Black *et al.* [14], Moreno *et al.* [30] and Harayama *et al.* [31], biphenyl coupling in *ortho*-position next to a sterically demanding residue such as *O*-benzyl or methoxy groups is possible. In contrast, the results of Vila and Dyke [32, 33] confirm our findings. As the results of Harayama *et al.* [34] and Kirst [28] show, the addition of a phosphine ligand as well as preactivation of the coupling site are necessary if palladium is to act as a catalyst rather than a reactant. It should be noted that the preparation of starting materials where the positions to be coupled are activated give higher net yields [35] than without activation.

2.3. Structure elucidation of oxoassoanine (2c)

To the best of our knowledge, the crystal structure of **2c** is hitherto unknown. Structural knowledge of pyrrolophenanthridone alkaloids in general, as revealed by a search of the Cambridge Structural Database (CSD) [36] *via* the WebCSD interface [37] in September 2018, is still rather limited. Merely a crystal structure of pratorinine has long been known [38]. More recently, crystal structures of lycoranine A and B were reported [39].

The spectroscopic data obtained for **2c** are in agreement with those reported in the literature [28, 34]. The structure was unambiguously revealed by single-crystal X-ray analysis. Crystals of **2c** suitable for single-crystal X-ray diffraction were obtained from a solution in dimethylformamide using the slow-evaporation method. Compound **2c** crystallizes in the orthorhombic space group *Pnma* with four molecules in the unit cell. In the crystal, the molecular plane of **2c** lies on a crystallographic mirror plane parallel to (010) at $y = 1/4$. The flat molecule thus exhibits exact C_S symmetry in the crystal (Figure 7a). The slightly elongated anisotropic atomic displacement of C4, C5, C12 and C13 perpendicular to the crystallographic mirror plane indicate that the dihydropyrrole ring is actually slightly non-planar and the methyl groups are slightly displaced from the mirror plane. The methoxy groups are thus approximately coplanar with the benzene ring resulting in local C_{2v} symmetry of the dimethyoxybenzene moiety, as observed for **1c**, **1f** and **1g** (see Section 2.1). The space group *Pnma* is among those providing maximum density packing of C_S-symmetric molecules where the molecule retains inherent symmetry [40]. Figure 7b shows a limitingly close-packed layer, *i.e.* a close-packed layer in which the molecule occupies a special position [41], parallel to the (010) plane in the crystal structure of **2c**. These layers stack in the *b* axis direction in an AB sequence, where A and B are rotated to one another by 180°. The stacking distance between the layers corresponds to *b*/2 (3.36 Å). A Kitajgorodskij packing index [40] of 75.8 % indicates a remarkably dense crystal packing. By comparison, the packing index calculated for the related pratorinine (CSD refcode: DIBHUR) [38], whose crystal structure features 1D hydrogen-bonded zigzag chains along 2_1 screw axes (space group $P2_1/n$), formed by hydrogen bonds between the hydroxy group bonded to C10 of the pyrrolophenanthridone scaffold and the carbonyl oxygen atom of adjacent molecules, is 73.1 %. In contrast to **2c**, the crystal structures of the related lycoranine A (CSD refcode: BIGXOG) and B (CSD refcode: BIGXUM) [39] both exhibit a herringbone pattern (space group $P2_12_12_1$) with packing indices of 73.2 and 74.1 %, respectively.

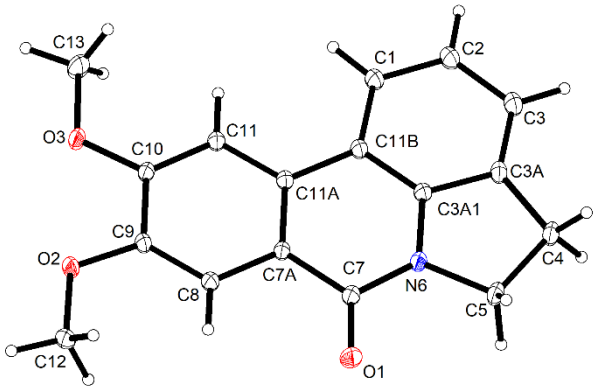

(a)

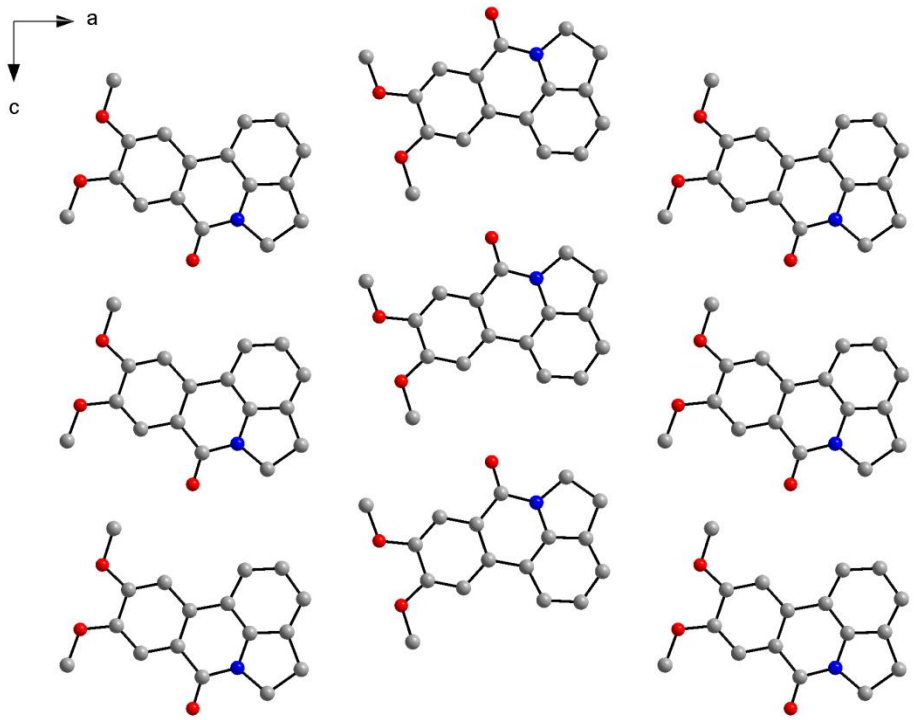

(b)

Figure 7 (a) Molecular structure of **2c** in the crystal. Displacement ellipsoids are drawn at the 50 % probability level. H atoms are represented by small spheres of arbitrary radii. (b) Section of a close-packed layer in the crystal structure of **2c** viewed along the *b* axis direction. H atoms are omitted for clarity.

3. Conclusions

The results reported here extend the intramolecular coupling reactions of *N*-acylindolines to pyrrolophenanthridone alkaloids. We prepared and subjected seven substituted *N*-acylindolines to Pd(II)-mediated arylation. Depending on the substitution pattern of the two aromatic components, at best a mixture of coupling products was isolated and characterized. Crystal structure analyses of the precursors and alkaloids studied established conformational preferences. Both phenyl rings need to bear electron-donating substituents for successful ring coupling. It was not possible to prevent the formation of oxidized products and elementary palladium. The yield of the desired scaffold was always relatively low and formation of similar products could not be prevented. While it appears attractive because it is straightforward, the Pd(II)-mediated coupling of *N*-acylindolines can only be recommended if a mixture of products can be tolerated. Using this method, we synthesised oxoassoanine and successfully determined its crystal structure.

4. Experimental section

4.1. General

Reagent grade starting materials and solvents were purchased and used as received without further purification. Analytical TLC was performed on Siliga gel 60 F_{254} TLC plates (Merck KGaA, Darmstadt). Reported R_f values are uncorrected. Column chromatography was conducted with Merck Silica gel 60 (40-63 µm) and flash chromatography with puriFlash® (30 µm silica gel, 60 Å - 500 m^2 g^{-1}) columns (Interchim, Monteluçon, France). Melting points (uncorrected) were determined on a Boetius melting point apparatus (VEB Kombinat NAGEMA, Dresden, GDR). Infrared (IR) spectra were recorded on a Bruker (Billerica, Massachusettes, USA) IFS 28 FTIR spectrometer equipped with a Thermo Spectra-Tech attenuated total reflection (ATR) unit (Thermo Scientific, Waltham, Massachusetts, USA) with a 20 mm ZnSe-Fresnel crystal. The angle of incidence was 45°. High resolution mass spectra (HRMS) were measured on a LTQ-Orbitrap-XL (ESI source) of Thermo Scientific. Samples were dissolved in chloroform / methanol.

4.2. NMR spectroscopy

^{1}H and ^{13}C NMR spectra were recorded on a Varian (now Agilent Technologies, Böblingen, Germany) Inova 500 MHz or an Agilent Technologies VNMRS 400 MHz spectrometer. Chemical shifts (δ) are reported relative to TMS, using residual solvent peaks as internal standards: acetic acid-*d*4: δ_H = 2.04 ppm, δ_C = 20.00 ppm; acetone-*d*6: δ_H = 2.04 ppm, δ_C = 29.92 ppm; benzene-*d*6: δ_H = 7.16 ppm; chloroform-*d* ($CDCl_3$): δ_H = 7.26 ppm, δ_C = 77.23 ppm. Abbreviations: singlet (s), broad singlet (bs), doublet (d), doublet of doublets (dd), doublet of doublet of doublets (ddd), doublet of triplet (dt), triplet (t), quartet (q), multiplet (m). Variable-temperature ^{1}H NMR measurements were carried out using a standard Varian L900 variable-temperature controller.

4.3. X-ray crystallography

Crystals suitable for single-crystal X-ray analysis were selected with the aid of a polarising microscope, mounted on a MiTeGen cryo loop using perfluoropolyether PFO-XR75 and placed in the nitrogen cold gas stream of the diffractometer. The X-ray intensity data for **1a** and **1e** were collected on the P11 beamline at the PETRA III light source (DESY, Hamburg) at an X-ray energy of 22.0 keV. The primary beam intensity was monitored continuously and stored during the experiment. The P11 X-ray optics consisted of a liquid nitrogen-cooled Si(111) and Si(113) double-crystal monochromator and one vertical and two horizontal deflecting X-ray mirrors. The source brilliance at the crystal was 1.7×10^{12} photons per s. The data were collected using a 50 μm beam on a PILATUS 6M-0109 detector (Dectris Ltd, Baden, Switzerland) [42] at a distance of 156 mm from the crystal. The 20-bit dynamic range of the PILATUS 6M detector allowed for collection of weak high-order and stronger low-order reflections at the same time in one run. The crystal was rotated by 360° in steps of 0.5° with an exposure of 0.4 s per frame using the P11 Crystallography Control graphical user interface at the P11 beamlime [43]. The data were processed with the XDS program package [44]. The X-ray intensity data for **1b** and **1f** were collected on a Bruker AXS X8 Proteum diffractometer, using Cu-K_α radiation from a rotating anode X-ray source. The intensity data collections were carried out on a Bruker AXS Kappa APEX II diffractometer for **1d** and **2c**, using Mo-K_α radiation from a microfocus X-ray tube, and on an Enraf-Nonius Kappa CCD, using Mo-K_α radiation from a rotating anode X-ray source, for **1c** and **1g**. The crystal structures were solved with SHELXT [45] and refined with SHELXL [46]. Anisotropic displacement parameters were introduced for all non-hydrogen atoms. Hydrogen atoms were

placed at geometrically calculated positions and treated with an appropriate riding model. Crystal and molecular structures were drawn with DIAMOND [47]. CCDC 1827068-1827075 contain the supplementary crystallographic data for this paper. The data can be obtained free of charge from the Cambridge Crystallographic Data Centre via http://www.ccdc.cam.ac.uk/getstructures

Crystal data and refinement details

1a: $C_{16}H_{13}NO_3$, M_r = 267.27, triclinic, $P\bar{1}$, Z = 4, a = 7.530(2) Å, b = 10.867(2) Å, c = 15.914(2) Å, α = 88.958(6)°, β = 84.170(8)°, γ = 71.065(5)°, V = 1225.2(5) Å^3, T = 80(2) K, λ = 0.5636 Å, F(000) = 560, crystal size 0.040 × 0.039 × 0.029 mm, ρ_{calcd} = 1.449 mg m^{-3}, μ = 0.064 mm^{-1}, $2\theta_{max}$ = 53.60°, reflections collected / unique 33274 / 9715 (R_{int} = 0.0384), parameters 361, $R1[I > 2\sigma(I)]$ = 0.0629, $wR2$ (all data) = 0.2088, S = 1.149, residuals 0.776 / –0.472 e Å^{-3}. CCDC 1827068.

1b: $C_{16}H_{15}NO_2$, M_r = 253.29, monoclinic, $P2_1$, Z = 2, a = 4.6019(3) Å, b = 9.9484(6) Å, c = 13.6453(10) Å, β = 97.193(5)°, V = 619.79(7) Å^3, T = 100(2) K, λ = 1.54178 Å, F(000) = 268, crystal size 0.209 × 0.077 × 0.021 mm, ρ_{calcd} = 1.357 mg m^{-3}, μ = 0.719 mm^{-1}, $2\theta_{max}$ = 143.71°, reflections collected / unique 7059 / 2393 (R_{int} = 0.0748), parameters 173, $R1[I > 2\sigma(I)]$ = 0.0743, $wR2$ (all data) = 0.1970, S = 1.007, residuals 0.346 / –0.363 e Å^{-3}. CCDC 1827069.

1c: $C_{17}H_{17}NO_3$, M_r = 283.31, orthorhombic, $Pna2_1$, Z = 4, a = 7.469(2) Å, b = 22.036(10) Å, c = 8.507(2) Å, V = 1400.1(9) Å^3, T = 100(2) K, λ = 0.71073 Å, F(000) = 600, crystal size 0.290 × 0.060 × 0.040 mm, ρ_{calcd} = 1.344 mg m^{-3}, μ = 0.092 mm^{-1}, $2\theta_{max}$ = 63.68°, reflections collected / unique 25442 / 4803 (R_{int} = 0.1143), parameters 192, $R1[I > 2\sigma(I)]$ = 0.0645, $wR2$ (all data) = 0.1579, S = 1.074, residuals 0.433 / –0.490 e Å^{-3}. CCDC 1827070.

1d: $C_{18}H_{19}NO_4$, M_r = 313.34, triclinic, $P\bar{1}$, Z = 2, a = 6.4834(17) Å, b = 10.873(3) Å, c = 12.523(3) Å, α = 111.429(3)°, β = 99.886(4)°, γ = 101.268(4)°, V = 776.8(4) Å^3, T = 100(2) K, λ = 0.71073 Å, F(000) = 332, crystal size 0.294 × 0.206 × 0.094 mm, ρ_{calcd} = 1.340 mg m^{-3}, μ = 0.095 mm^{-1}, $2\theta_{max}$ = 70.00°, reflections collected / unique 43848 / 6844 (R_{int} = 0.0813), parameters 211, $R1[I > 2\sigma(I)]$ = 0.0599, $wR2$ (all data) = 0.1522, S = 1.074, residuals 0.451 / –0.346 e Å^{-3}. CCDC 1827071.

1e: $C_{23}H_{21}NO_3$, M_r = 359.41, monoclinic, $P2_1/c$, Z = 4, a = 17.094(3) Å, b = 14.083(3) Å, c = 7.3578(15) Å, β = 97.82(3)°, V = 1754.8(6) Å^3, T = 80(2) K, λ = 0.6199 Å, F(000) = 760, crystal size 0.064 × 0.047 × 0.034 mm, ρ_{calcd} = 1.360 mg m^{-3}, μ = 0.068 mm^{-1}, $2\theta_{max}$ = 53.67°, reflections collected / unique 72595 / 5570 (R_{int} = 0.0598), parameters 245, $R1[I > 2\sigma(I)]$ = 0.0405, $wR2$ (all data) = 0.1095, S = 1.043, residuals 0.555 / – 0.292 e Å^{-3}. CCDC 1827072.

1f: $C_{17}H_{16}N_2O_5$, M_r = 328.32, orthorhombic, $Pca2_1$, Z = 4, a = 23.1839(11) Å, b = 4.4220(2) Å, c = 14.3280(7) Å, V = 1468.90(12) Å^3, T = 100(2) K, λ = 1.54178 Å, F(000) = 688, crystal size 0.360 × 0.230 × 0.030 mm, ρ_{calcd} = 1.357 mg m^{-3}, μ = 0.719 mm^{-1}, $2\theta_{max}$ = 144.55°, reflections collected / unique 18733 / 2845 (R_{int} = 0.0423), parameters 220, $R1[I > 2\sigma(I)]$ = 0.0481, $wR2$ (all data) = 0.1347, S = 1.130, residuals 0.273 / –0.271 e Å^{-3}. CCDC 1827073.

1g: $C_{18}H_{16}F_3NO_3$, M_r = 351.32, monoclinic, $P2_1/c$, Z = 4, a = 8.8630(18) Å, b = 24.174(5) Å, c = 7.4029(15) Å, β = 100.11(3)°, V = 1561.5(6) Å^3, T = 100(2) K, λ = 0.71073 Å, F(000) = 728, crystal size 0.160 × 0.070 × 0.020 mm, ρ_{calcd} = 1.494 mg m^{-3}, μ = 0.125 mm^{-1}, $2\theta_{max}$ = 66.20°, reflections collected / unique 32134 / 5916 (R_{int} = 0.0965), parameters 228, $R1[I > 2\sigma(I)]$ = 0.0781, $wR2$ (all data) = 0.1343, S = 1.077, residuals 0.423 / –0.335 e Å^{-3}. CCDC 1827074.

2c: $C_{17}H_{15}NO_3$, M_r = 281.30, orthorhombic, $Pnma$, Z = 4, a = 22.426(3) Å, b = 6.7141(8) Å, c = 8.4025(10) Å, V = 1265.2(3) Å^3, T = 100(2) K, λ = 0.71073 Å, F(000) = 592, crystal size 0.171 × 0.092 × 0.041 mm, ρ_{calcd} = 1.477 mg m^{-3}, μ = 0.102 mm^{-1}, $2\theta_{max}$ = 66.46°, reflections collected / unique 36070 / 2604 (R_{int} = 0.0368), parameters 143, $R1[I > 2\sigma(I)]$ = 0.0400, $wR2$ (all data) = 0.1251, S = 1.088, residuals 0.574 / –0.267 e Å^{-3}. CCDC 1827075.

4.4 Syntheses

Benzo[d][1,3]dioxol-5-yl(indolin-1-yl)methanone (1a) [17-19]: Indoline (354 mg, 2.97 mmol) was dissolved in 16 mL of dichloromethane and triethylamine (342 mg, 3.375 mmol) was added. Subsequently, a solution of piperonoyl chloride (500 mg, 2.7 mmol) in 11 mL of dichloromethane was added dropwise while stirring and the resulting mixture was heated to reflux for 1 h. After cooling to room temperature, the reaction mixture was diluted with 10 mL of dichloromethane and washed with 1 N HCl (20 mL). The organic phase was separated and dried over $MgSO_4$. The solvent was then removed using a rotary evaporator.

The crude product was suspended in a small amount ethyl acetate / heptane (1:2) and filtered off to yield **1a** as an off-white solid (543 mg, 2.032 mmol, 75 %). Mp 121–122 °C; R_f = 0.32 (ethyl acetate / heptane 1:2); IR (ATR): 3070 (w), 2895 (w), 2780 (w), 1636 (s), 1594 (m), 1502 (m), 1478 (s),1462 (m), 1435 (s), 1383 (s), 1338 (m), 1320 (m), 1297 (m), 1245 (s), 1163 (w), 1103 (m), 1087 (w), 1033 (m), 923 (m), 872 (w), 811 (w), 753 (m) cm^{-1}; ^1H NMR: (400 MHz, $CDCl_3$): δ = 7.22 (d, 1H J = 7.4 Hz, Ind-H4), 7.11 (dd, J = 7.8 Hz, 1H, Phe-H4), 7.10-7.17 (br, 1H, Ind-H6), 7.06 (s, 1H, Phe-H6), 7.02 (t, J = 7.4 Hz, 1H, Ind-H5), 6.87 (d, J = 7.8 Hz, 1H, Phe-H3), 6.04 (s, 2H, O-CH_2-O), 4.12 (t, J = 8.1 Hz, 2 H, Ind-H2), 3.12 (t, J = 8.1 Hz, 2H, Ind-H3) ppm; $^{13}C\{^1H\}$ NMR (100 MHz, $CDCl_3$): δ = 168.2, 149.3, 147.6, 142.7, 132.4, 130.5, 127.1, 124.9, 123.7, 122.0, 116.7, 108.2, 108.1, 101.5, 50.8, 28.1 ppm; HRMS(ESI+): *m*/*z* calcd. for $C_{16}H_{14}NO_3$ $[M+H]^+$: 268.0974; found: 268.0969.

Indolin-1-yl(4-methoxyphenyl)methanone (1b) [16, 20, 21]: 1b was prepared from indoline (354 mg, 2.97 mmol) and *p*-anisoyl chloride (4-methoxybenzoyl chloride; 461 mg, 2.7 mmol) analogously to **1a**. Recrystallization from ethanol afforded colourless crystals of **1b** (533 mg, 2.104 mmol, 78 %). Mp 108-110 °C; R_f = 0.21 (ethyl acetate / heptane 1:2); IR (ATR): 3042 (w), 2958 (w), 2837 (w), 1637 (s), 1606 (s), 1597 (m), 1574 (w), 1511 (m), 1481 (s), 1462 (m), 1441 (w), 1388 (s), 1342 (m), 1322 (w), 1299 (m), 1252 (s), 1174 (m), 1155 (w), 1110 (w), 1028 (w), 840 (w), 759 (w) cm^{-1}; ^1H NMR: (400 MHz, $CDCl_3$): δ = 7.55 (m, 2H, Phe-H2, H6), 7.21 (d, J = 7.3 Hz, 1H, Ind-H4), 7.07-7.16 (m, 1H, Ind-H6), 7.00 (t, J = 7.2 Hz, 1H, Ind-H5), 6.94 (m, 2H, Phe-H3,H5), 4.12 (t, J = 8.2 Hz, 2H, Ind-H2), 3.86 (s, 3H, OCH_3), 3.110 (t, J = 8.22 Hz, 2H, Ind-H3) ppm; ^1H NMR (500 MHz, acetone-*d*6): δ = 7.74 (bs, 1H, Ind-H7), 7.63-7.56 (m, 2H, Phe-H2,H6), 7.25 (dt, J = 7.5, 1.4 Hz, 1H, Ind-H4), 7.14 (t, J = 7.9 Hz, 1H, Ind-H6), 7.07-6.97 (m, 3H, Phe-H3,H5, Ind-H5), 4.11 (t, J = 8.4, 1.6 Hz, 2H, Ind-H2), 3.89 (s, 3H, OCH_3), 3.12 (t, J = 8.3 Hz, 2H, Ind-H3) ppm; ^1H NMR: (500 MHz, acetic acid-*d*4, 70° C): δ = 7.55-7.62 (m, 2H, Phe-H2,H6), 7.52 (bs, 1H, Ind-H7), 7.23 (ddq, J = 7.5, 1.7, 0.8 Hz, 1H, Ind-H4), 7.12 (t, J = 7.6 Hz, 1H, Ind-H6), 7.07-6.98 (m, 3H, Phe-H3,H5, Ind-H5), 4.14 (t, J = 8.2 Hz, 2H, Ind-H2), 3.88 (s, 3H, OCH_3), 3.12 (t, J = 8.2 Hz, 2H, Ind-H3) ppm; $^{13}C\{^1H\}$ NMR (100 MHz, $CDCl_3$): δ = 168.8, 161.3, 142.4, 132.4, 129.3 (2 × C), 129.1, 127.1, 124.9, 123.6, 116.8, 113.7 (2 × C), 55.4, 50.7, 28.2 ppm; HRMS(ESI+): *m*/*z* calcd. for $C_{16}H_{16}NO_2$ $[M+H]^+$: 254.1181; found: 254.1179.

(3,4-dimethoxyphenyl)(indolin-1-yl)methanone (1c): Veratric acid (3,4-dimethoxy-benzoic acid; 13.912 g, 76.29 mmol) and thionyl chloride (71 mL, 0.979 mol) were heated to reflux for 2 h. Subsequently, excess thionyl chloride was removed under reduced pressure and the residue was taken up in a small amount of dichloromethane and again evaporated to dryness. The acid chloride so obtained was redissolved in 230 mL of dichloromethane and added dropwise to a solution of indoline (10 g, 83.92 mmol) and triethylamine (9.65 g, 95.4 mmol) in 250 mL of dichloromethane at 0 °C under argon. The reaction mixture was then heated to reflux for 20 min. After cooling to room temperature, the mixture was concentrated to 290 mL and washed with 1 N HCl (290 mL). The organic phase was separated and aqueous phase was re-extracted three times with dichloromethane. The combined organic layers were dried over $MgSO_4$ and the solvent was removed using a rotary evaporator. The crude product was recrystallized from ethanol to afford colourless needles of **1c** (19.35 g, 68.29 mmol, 90 %). Mp 133–135 °C; R_f = 0.44 (ethyl acetate/heptane 7:3); IR(ATR): 3000 (w), 2958 (w), 2935 (w), 2837 (w), 1638 (s), 1598 (m), 1582 (m), 1514 (m), 1481 (s), 1462 (m), 1415 (s), 1386 (s), 1340 (m), 1321 (m), 1298 (w), 1263 (s), 1245 (m), 1229 (m), 1176 (w), 1139 (m), 1024 (m), 934 (w), 756 (w) cm^{-1}; ^1H NMR: (400 MHz, $CDCl_3$): δ = 7.21 (dp, J = 7.4 Hz, 1.0 Hz, 1H, Ind-H4), 7.16 (dd, J = 8.1, 1.9 Hz, 1H, Phe-H6), 7.14 (s, 1H, Phe-H2), 7.11 (bs, 1H, Ind-H6), 7.04–6.95 (m, 1H, Ind-H5), 6.89 (d, J = 8.2 Hz, 1H, Phe-H5), 4.13 (t, J = 8.2 Hz, 2H, Ind-H3), 3.93 (s, 3H, OCH_3), 3.89 (s, 3H, OCH_3), 3.12 (t, J = 8.2 Hz, 2H, Ind-H3) ppm; $^{13}C\{^1H\}$ NMR (100 MHz, $CDCl_3$): δ = 168.7, 150.9, 149.0, 142.8, 132.4, 129.2, 127.1, 124.9, 123.7, 120.5, 116.7, 110.9, 110.6, 56.0 (2 × C), 50.7, 28.1 ppm; HRMS (ESI+): calcd. $C_{17}H_{18}NO_3$ = 284.1281 $[M+H]^+$; found: 284.1286.

Indolin-1-yl(3,4,5-trimethoxyphenyl)methanone (1d): indoline (1.14 g, 9.53 mmol) and triethylamine (1.14 g, 10.80 mmol) were dissolved in 60 mL of dichloromethane. Subsequently, a solution of 3,4,5-trimethoxybenzoyl chloride (2.00 g, 8.67 mmol) in 30 mL of dichloromethane was added dropwise while stirring and the resulting mixture was heated to reflux for 1 h. After cooling to room temperature, the reaction mixture was diluted with 10 mL of dichloromethane and washed with 1 N HCl (80 mL). The organic phase was separated and dried over $MgSO_4$. The solvent was then removed using a rotary evaporator. The crude product was recrystallized twice from ethanol to afford colourless crystals of **1d** (1.96 g, 6.25 mmol, 72 %). Mp 104-106 °C; R_f = 0.16 (ethyl acetate/heptane 1:2); IR(ATR): 2939 (w), 2836 (w), 1642 (m), 1583 (s), 1504 (w), 1481 (s), 1462 (m), 1412 (s), 1391 (s), 1345 (m), 1328 (w), 1295 (w), 1237 (m), 1180 (w), 1125 (s), 1004 (w), 760 (w) cm^{-1};

^{1}H NMR (400 MHz, $CDCl_3$): δ = 7.20 (dp, J = 7.3, 1.0 Hz, 1H, Ind-H4), 7.10 (bs, 1H, Ind-H6), 7.00 (t, J = 7.4 Hz, 1H, Ind-H5), 6.77 (s, 2H, Phe-H2,H6), 4.10 (t, J = 8.3 Hz, 2H, Ind-H2), 3.88 (s, 3H, OCH_3), 3.84 (s, 6H, 2 × OCH_3), 3.12 (t, J = 8.3 Hz, 2H, Ind-H3) ppm; ^{13}C{^{1}H} NMR (100 MHz, $CDCl_3$): δ = 153.3, 142.5, 139.8, 132.4, 132.1, 127.2, 124.9, 123.9, 117.0, 101.5, 60.9, 56.3, 50.5, 28.1 ppm; HRMS(ESI+): m/z calcd. for $C_{18}H_{20}NO_4$ $[M+H]^+$: 314.1393; found: 314.1387.

[4-(benzyloxy)-3-methoxyphenyl](indolin-1-yl)methanone (1e): 4-(benzyloxy)-3-methoxybenzoic acid (217 mg, 0.84 mmol) and thionyl chloride (15 mL, 0.207 mol) were heated to reflux for 2 h. Subsequently, excess thionyl chloride was removed under reduced pressure and the residue was taken up in a small amount of dichloromethane and again evaporated to dryness. The acid chloride so obtained was redissolved in 10 mL of dichloromethane and added dropwise to a stirred solution of indoline (100 mg, 0.85 mmol) and triethylamine (9.65 g, 95.4 mmol) in 10 mL of dichloromethane. The reaction mixture was then heated to reflux for 20 min. After cooling to room temperature, the solvent was removed using a rotary evaporator. The crude product was purified by flash chromatography using ethyl acetate / heptane (4:6) as solvent to yield **1e** as an off-white solid (267 mg, 0.74 mmol, 88 %). Mp 153–156 °C; R_f = 0.36 (ethyl acetate / *n*-heptane 4:6); IR(ATR): 3031 (w), 2935 (w), 2907 (w), 2838 (w), 1638 (s), 1597 (m), 1581 (m), 1512 (m), 1480 (s), 1462 (m), 1415 (s), 1385 (s), 1339 (m), 1321 (m), 1263 (s), 1221 (m), 1178 (w), 1137 (m), 1023 (w), 868 (w), 813 (w), 753 (w), 697 (w) cm^{-1}; ^{1}H NMR (500 MHz, $CDCl_3$) δ = 7.45 (ddq, J = 7.0, 1.3, 0.7 Hz, 2H, Bn-H), 7.40–7.35 (m, 2H, Bn-H), 7.34-7.29 (m, 1H, Bn-H), 7.20 (dp, J = 7.3, 1.0 Hz, 1H, Ind-H4), 7.16 (s, 1H, Phe-H2), 7.10 (bs, 1H, Ind-H6), 7.08 (dd, J = 8.2, 2.0 Hz, 1H, Phe-H6), 7.02–6.97 (m, 1H, Ind-H5), 6.91 (d, J = 8.2 Hz, 1H, Phe-H5), 5.20 (s, 2H, OCH_2-Bn), 4.11 (t, J = 8.2 Hz, 2H, Ind-H2), 3.89 (s, 3H, OCH_3), 3.10 (t, J = 8.4 Hz, 2H, Ind-H3) ppm; ^{13}C{^{1}H} NMR (101 MHz, $CDCl_3$): 168.6, 150.0, 149.6, 142.8, 136.6, 132.4, 129.7, 128.6, 128.0, 127.3,, 127.1, 124.9, 123.7, 120.3, 116.8, 113.1, 111.4, 71.0, 56.1, 50.7, 28.1 ppm; HRMS(ESI+): m/z calcd. for $C_{23}H_{22}NO_3$ $[M+H]^+$: 360.1600, found: 360.1601; m/z calcd. for $C_{23}H_{21}NNaO_3$ $[M+H]^+$: 382.1419; found: 382.1424.

(3,4-dimethoxyphenyl)(6-nitroindolin-1-yl)methanone (1f): Veratric acid (3,4-dimethoxybenzoic acid; 303 mg, 1.66 mmol) and thionyl chloride (360 µL, 4.96 mmol) were dissolved in 15 mL of toluene and heated to reflux for 2 h. Subsequently, excess thionyl

chloride was removed under reduced pressure and the residue was taken up in a small amount of dichloromethane and again evaporated to dryness. The acid chloride so obtained was redissolved in 5 mL of dichloromethane and added dropwise to a stirred solution of 6-nitroindoline (300 mg, 1.83 mmol) and triethylamine (210 mg, 2.08 mmol) in 10 mL of dichloromethane. The reaction mixture was further stirred for 1 h at room temperature and the solvent was then removed using a rotary evaporator. Recrystallization from ethanol afforded amber crystals of **1f** (371 mg, 1.13 mmol, 68 %). Mp 181-183 °C; R_f = 0.42 (ethyl acetate / *n*-heptane 1:2); IR(ATR): 2934 (w), 2838 (w), 1645 (m), 1598 (m), 1582 (m), 1517 (s), 1480 (m), 1414 (m), 1386 (s), 1337 (s), 1263 (s), 1239 (m), 1177 (m), 1140 (m), 1023 (w), 888 (w), 809 (w), 740 (w) cm^{-1}; ^1H NMR (500 MHz, $CDCl_3$) δ = 8.52 (bs, 1H, Ind-H7), 7.92 (dd, *J* = 8.2, 2.2 Hz, 1H), 7.32 (dt, *J* = 8.2, 1.1 Hz, 1H), 7.21-7.14 (m, 2H), 6.92 (d, *J* = 8.1 Hz, 1H), 4.24 (t, *J* = 8.4 Hz, 2H, Ind-H2), 3.95 (s, 3H, OCH_3), 3.92 (s, 3H, OCH_3), 3.26–3.18 (m, 2H, Ind-H3) ppm; $^{13}C\{^1H\}$ NMR (100 MHz, $CDCl_3$) δ = 169.0, 151.4, 149.1, 147.8, 144.1, 139.6, 128.1, 124.8, 120.5, 119.3, 112.1, 110.9, 110.6, 56.1 (2 × C), 51.4, 28.3 ppm. HRMS(ESI+): *m*/*z* calcd. for $C_{17}H_{17}N_2O_5$ $[M+H]^+$: 329.1138; found: 329.1142; *m*/*z* calcd. for $C_{17}H_{16}N_2NaO_5$ $[M+Na]^+$: 351.0957; found: 351.0961.

(3,4-dimethoxyphenyl)(6-(trifluoromethyl)indolin-1-yl)methanone (1g): Veratric acid (3,4-dimethoxybenzoic acid; 213 mg, 1.16 mmol) and thionyl chloride (1.27 mL, 17.51 mmol) were dissolved in 6 mL of toluene and heated to reflux for 2 h. Subsequently, excess thionyl chloride was removed under reduced pressure and the residue was taken up in a small amount of dichloromethane and again evaporated to dryness. The acid chloride so obtained was redissolved in 5 mL of dichloromethane and added dropwise to a stirred solution of 6-trifluoromethyl indoline (240 mg, 1.28 mmol) and triethylamine (148 mg, 1.45 mmol) in 10 mL of dichloromethane. The reaction mixture was further stirred over night at room temperature and the solvent was then removed using a rotary evaporator. Recrystallization from ethanol afforded colourless crystals of **1g (**298 mg, 0.85 mmol, 73 %). Mp 139-140°C; R_f = 0.38 (ethyl acetate / *n*-heptane 1:1); IR(ATR): 3005 (w), 2937 (w), 2839 (w), 1642 (w), 1603 (m), 1582 (m), 1514 (m), 1498 (m), 1433 (m), 1415 (s), 1385 (s), 1333 (m), 1314 (s), 1259 (s), 1242 (m), 1159 (m), 1138 (m), 1115 (s), 1078 (m), 1056 (m), 1024 (m), 944 (w), 889 (w), 818 (w),752 (w) cm^{-1}; ^1H NMR (500 MHz, $CDCl_3$): δ = 7.97 (bs, 1H, Ind-H7), 7.29 (d, *J* = 1.5 Hz, 2H), 7.19-7.13 (m, 2H), 6.91 (d, *J* = 8.1 Hz, 1H), 4.18 (t, *J* = 8.4 Hz, 2H, Ind-H2), 3.94 (s, 3H, OCH_3), 3.90 (s, 3H, OCH_3), 3.17 (t, *J* = 8.3 Hz, 2H, Ind-H3) ppm; $^{13}C\{^1H\}$ NMR (100 MHz, $CDCl_3$): δ = 168.9, 151.2, 149.1, 143.5, 136.2, 129.8 (q, *J* = 32.1 Hz),

128.5, 124.9, 124.1 (q, J = 272.6 Hz), 120.7, 120.5, 114.1, 110.9, 110.5, 56.0, 51.0, 28.2 ppm; HRMS(ESI+): m/z calcd. $C_{18}H_{17}F_3NO_3$ $[M+H]^+$: 352.1161; found: 352.1165; m/z calcd. $C_{18}H_{16}F_3NNaO_3$ $[M+Na]^+$: 374.0980; found: 374.0986.

Oxoassoanine (2c): 1c (300 mg, 1.06 mmol) was dissolved in glacial acetic acid and palladium(II) acetate (238 mg, 1.06 mmol) was added. The mixture was heated to reflux for 5 h. After cooling to room temperature, the palladium precipitate was removed by filtration. The solvent was removed using a rotary evaporator and the resulting residue was subjected to column chromatography eluting with chloroform / methyl *tert*-butyl ether. **2c** eluted as the third fraction to give an off-white powder (93 mg, 0.33 mmol, 32 %). Mp 274-275 °C; R_f = 0.41 (ethyl acetate / *n*-heptane 7:3); IR(ATR): 3058 (w), 3009 (m), 2920 (w), 2837 (w), 1724 (w), 1643 (s), 1625 (w), 1605 (s), 1520 (w), 1479 (m), 1436 (w), 1389 (w), 1363 (w), 1301 (w), 1272 (w), 1233 (w), 1208 (w), 1122 (w), 1065 (w), 1028 (w), 869 (w), 761 (m), 742 (w) cm^{-1}; ^1H NMR (400 MHz, $CDCl_3$): δ = 8.14 (d, J = 8.02 Hz, 1H), 7.95 (s, 1H), 7.55 (s, 1H), 7.30 (dd, J = 7.238 Hz, 1H), 7.21 (t, J = 7.238 Hz, 1H), 4.50 (t, J = 8.021 Hz, 2H, Ind-H2), 4.09 (s, 3H, OCH_3), 4.05 (s, 3H, OCH_3), 3.44 (t, J = 8.216 Hz, 2H, Ind-H3) ppm; ^{13}C NMR (100 MHz, $CDCl_3$): δ = 163.9, 157.0, 153.5, 142.7, 135.0, 132.7, 127.9, 127.5, 124.5, 123.1, 120.7, 112.2, 106.9, 59.9, 50.4, 31.2 ppm; HRMS(ESI+): m/z calcd. for $C_{17}H_{16}NO_3$ $[M+H]^+$: 282.1130; found: 282.1132.

8,9-dimethoxy-6*H*-isoindolo[2,1-*a*]indol-6-one (4c): 4c was isolated as yellow needles from the first fraction during the chromatographic separation of **2c**. Yield: 37 mg (12 %). Mp 128-130 °C; R_f = 0.61 (ethyl acetate / heptane 7:3); IR(ATR): 2924(m), 2853 (w), 1730 (s), 1613 (m), 1493 (m), 1471 (m), 1448 (m), 1424 (w), 1338 (w), 1333 (w), 1314 (w), 1272 (m), 1216 (m), 1192 (w), 1147 (w), 1087 (m), 999 (w), 800 (w), 768 (w), 743 (w) cm^{-1}; ^1H NMR (400 MHz, $CDCl_3$): δ = 7.79 (dq, J = 8.0, 0.8 Hz, 1H), 7.37 (dt, J = 7.8, 0.9 Hz, 1H), 7.22 (ddd, J = 7.9, 7.4, 1.2 Hz, 1H), 7.19 (s, 1H), 7.11-7.05 (m, 1H), 6.94 (s, 1H), 6.42 (s, 1H), 3.96 (s, 3H, OCH_3), 3.92 (s, 3H, OCH_3) ppm; $^{13}C\{^1H\}$ NMR (126 MHz, $CDCl_3$): δ = 56.4 (2 × C), 102.4, 104.0, 107.6, 112.8, 122.0, 123.4, 126.1, 126.3, 129.0, 134.0, 134.5, 139.0, 150.1, 153.9, 162.8 ppm. HRMS(ESI+): m/z calcd. for $C_{17}H_{14}NO_3$ $[M+H]^+$: 280.0974; found: 280.0967; m/z calcd. for $C_{17}H_{13}NNaO_3$ $[M+Na]^+$: 302.0793; found: 302.0787. The second fraction during the chromatographic separation of **2c** was identified as unreacted **1c** (55 mg, 0.194 mmol, 18 %).

Acknowledgements

We would like to thank Heike Schucht, Elke Dreher and Nils Nöthling (Mülheim an der Ruhr, Germany) for assistance with the X-ray intensity data collections, Dr Dieter Ströhl (Halle, Germany) for performing the variable-temperature NMR experiments and Antje Herbrich-Peters (Halle, Germany) for recording the HRMS spectra. Parts of this research were carried out at the light source PETRA III at DESY, a member of the Helmholtz Association (HGF). Thanks are due to Dr Anja Burkhardt (Hamburg, Germany) for assistance in using beamline P11. Professor Christian W. Lehmann (Mülheim an der Ruhr, Germany) is gratefully acknowledged for his support of this project.

Supporting Information

^{1}H and ^{13}C NMR spectra of amides **1a-g**, and isolated products **2a**/**3a**, **2b**, **2c**, **4a**/**5a** oxidized **1b** and **4c**.

References

[1] The Plant List (2013). Version 1.1. Published on the Internet; http://www.theplantlist.org/ (accessed 19 st September).
[2] H. Tarun, D.-P. Isabel, Heterocyclic Amaryllidaceae Alkaloids: Biosynthesis and Pharmacological Applications, Current Topics in Medicinal Chemistry 17(4) (2017) 418-427.
[3] J.M. Llabrés, F. Viladomat, J. Bastida, C. Codina, M. Rubiralta, Phenanthridine alkaloids from Narcissus assoanus, Phytochemistry 25(11) (1986) 2637-2638.
[4] S. Ghosal, K.S. Saini, A.W. Frahm, Alkaloids of Crinum latifolium, Phytochemistry 22(10) (1983) 2305-2309.
[5] C. Fennell, J. Van Staden, Crinum species in traditional and modern medicine, Journal of Ethnopharmacology 78(1) (2001) 15-26.
[6] R.E. Hayden, G. Pratt, M.T. Drayson, C.M. Bunce, Lycorine sensitizes CD40 ligand-protected chronic lymphocytic leukemia cells to bezafibrate-and medroxyprogesterone acetate-induced apoptosis but dasatanib does not overcome reported CD40-mediated drug resistance, haematologica 95(11) (2010) 1889-1896.
[7] D. Lamoral-Theys, C. Decaestecker, V. Mathieu, J. Dubois, A. Kornienko, R. Kiss, A. Evidente, L. Pottier, Lycorine and its derivatives for anticancer drug design, Mini reviews in medicinal chemistry 10(1) (2010) 41-50.
[8] Y. Li, J. Liu, L.-J. Tang, Y.-W. Shi, W. Ren, W.-X. Hu, Apoptosis induced by lycorine in KM3 cells is associated with the G0/G1 cell cycle arrest, Oncology reports 17(2) (2007) 377-384.
[9] X.-s. Liu, J. Jiang, X.-y. Jiao, Y.-e. Wu, J.-h. Lin, Y.-m. Cai, Lycorine induces apoptosis and down-regulation of Mcl-1 in human leukemia cells, Cancer letters 274(1) (2009) 16-24.

[10] K.K. Schrader, F. Avolio, A. Andolfi, A. Cimmino, A. Evidente, Ungeremine and Its Hemisynthesized Analogues as Bactericides against Flavobacterium columnare, Journal of Agricultural and Food Chemistry 61(6) (2013) 1179-1183.
[11] A. Evidente, A. Andolfi, A.H. Abou-Donia, S.M. Touema, H.M. Hammoda, E. Shawky, A. Motta, (−)-Amarbellisine, a lycorine-type alkaloid from Amaryllis belladonna L. growing in Egypt, Phytochemistry 65(14) (2004) 2113-2118.
[12] J. He, W.B. Qi, L. Wang, J. Tian, P.R. Jiao, G.Q. Liu, W.C. Ye, M. Liao, Amaryllidaceae alkaloids inhibit nuclear- to- cytoplasmic export of ribonucleoprotein (RNP) complex of highly pathogenic avian influenza virus H5N1, Influenza and other respiratory viruses 7(6) (2013) 922-931.
[13] L. Szlávik, Á. Gyuris, J. Minárovits, P. Forgo, J. Molnár, J. Hohmann, Alkaloids from Leucojum vernum and antiretroviral activity of Amaryllidaceae alkaloids, Planta medica 70(09) (2004) 871-873.
[14] D.S.C. Black, P.A. Keller, N. Kumar, A direct synthesis of pyrrolophenanthridone alkaloids, Tetrahedron letters 30(42) (1989) 5807-5808.
[15] D.S.C. Black, P.A. Keller, N. Kumar, Synthesis of pyrrolophenanthridones by aryl-aryl coupling reactions, Tetrahedron 49(1) (1993) 151-164.
[16] M. Kim, N.K. Mishra, J. Park, S. Han, Y. Shin, S. Sharma, Y. Lee, E.K. Lee, J.H. Kwak, I.S. Kim, Decarboxylative acylation of indolines with alpha-keto acids under palladium catalysis: a facile strategy for the synthesis of 7-substituted indoles, Chem Commun (Camb) 50(91) (2014) 14249-52.
[17] T. Harayama, H. Toko, A. Hori, T. Miyagoe, T. Sato, H. Nishioka, H. Abe, Y. Takeuchi, Synthetic studies on pyrrolophenanthridone skeleton from 1-benzoyl-7-iododihydroindole derivatives using palladium-assisted biaryl coupling reactions, Heterocycles 61 (2003) 513-+.
[18] M.D. Ganton, M.A. Kerr, A domino amidation route to indolines and indoles: Rapid syntheses of anhydrolycorinone, hippadine, oxoassoanine, and pratosine, Org. Lett. 7(21) (2005) 4777-4779.
[19] A. Kumar, H.K. Akula, M.K. Lakshman, Simple Synthesis of Amides and Weinreb Amides via Use of PPh3 or Polymer-Supported PPh3 and Iodine, European J Org Chem 2010(14) (2010).
[20] T. Fang, X.H. Gao, R.Y. Tang, X.G. Zhang, C.L. Deng, A novel Pd-catalyzed N-dealkylative carbonylation of tertiary amines for the preparation of amides, Chem Commun (Camb) 50(94) (2014) 14775-7.
[21] L. Ren, X. Li, N. Jiao, Dioxygen-Promoted Pd-Catalyzed Aminocarbonylation of Organoboronic Acids with Amines and CO: A Direct Approach to Tertiary Amides, Org Lett 18(22) (2016) 5852-5855.
[22] F.K. Winkler, J.D. Dunitz, The Non-planar Amide Group, J. Mol. Biol. 59(1) (1971) 169-&.
[23] C. Vande Velde, E. Bultinck, K. Tersago, C. Van Alsenoy, F. Blockhuys, From anisole to 1,2,4,5-tetramethoxybenzene: Theoretical study of the factors that determine the conformation of methoxy groups on a benzene ring, Int. J. Quantum Chem. 107(3) (2007) 670-679.
[24] J.W. Emsley, E.K. Foord, J.C. Lindon, Continuous bond rotation models for the conformational analysis of the methoxy groups in 1,2-dimethoxy- and 1,2,3-trimethoxy-benzene using dipolar couplings obtained from the NMR spectra of oriented samples in nematic liquid crystalline solutions, J. Chem. Soc.-Perkin Trans. 2 (5) (1998) 1211-1218.
[25] V. Dupray, Recrystallization of Enantiomers from Conglomerates, in: K. Sztwiertnia (Ed.), Recrystallization, InTech2012, pp. 403-424.
[26] K. Nagarajan, M.D. Nair, P.M. Pillai, CONFIGURATION OF AMIDE BOND IN N-ACYLINDOLINES AND N-ACYLTETRAHYDROQUINOLINES, Tetrahedron 23(4) (1967) 1683-1690.
[27] R.J. Abraham, N.J. Ainger, Proton chemical shifts in NMR. Part 13. Proton chemical shifts in ketones and the magnetic anisotropy and electric field effect of the carbonyl group, J. Chem. Soc.-Perkin Trans. 2 (3) (1999) 441-448.
[28] J. Kirst, Synthese halogenierter Carbazole und Totalsynthese der Amaryllisalkaloide Pratosin und Hippadin, TU Dresden, 2009.
[29] T. Itahara, Intramolecular Ring Closure of 1-Aroylindoles by Palladium Acetate, Synthesis 1979(02) (1979) 151-152.
[30] I. Moreno, I. Tellitu, J. Etayo, R. SanMartín, E. Domínguez, Novel applications of hypervalent iodine: PIFA mediated synthesis of benzo[c]phenanthiridines and benzo[c]phenanthridinones, Tetrahedron 57(25) (2001) 5403-5411.

[31] T. Harayama, Y. Kawata, C. Nagura, T. Sato, T. Miyagoe, H. Abe, Y. Takeuchi, Effect of oxygen substituents on the regioselectivity of the Pd-assisted biaryl coupling reaction of benzanilides, Tetrahedron Letters 46(36) (2005) 6091-6094.
[32] J. Vila, A. Suarez, M. Pereira, E. Gayoso, M. Gayoso, Cyclometallation&—III. Regioselectivity in Pd (II) Cyclometallated complexes, Polyhedron 6(5) (1987) 1003-1007.
[33] N. Barr, S.F. Dyke, Palladium assisted organic reactions: III. The preparation of di-μ-chlorobis-(N, N-dialkylbenzylamine-2, C, N) dipalladium (II) complexes, Journal of Organometallic Chemistry 243(2) (1983) 223-232.
[34] T. Harayama, A. Hori, H. Abe, Y. Takeuchi, Concise synthesis of pyrrolophenanthridine alkaloids using a Pd-mediated biaryl coupling reaction with regioselective C–H activation via the intramolecular coordination of the amine to Pd, Tetrahedron 60(7) (2004) 1611-1616.
[35] U.V. Mentzel, D. Tanner, J.E. Tønder, Comparative Study of the Kumada, Negishi, Stille, and Suzuki−Miyaura Reactions in the Synthesis of the Indole Alkaloids Hippadine and Pratosine, The Journal of Organic Chemistry 71(15) (2006) 5807-5810.
[36] C.R. Groom, I.J. Bruno, M.P. Lightfoot, S.C. Ward, The Cambridge Structural Database, Acta Crystallogr B Struct Sci Cryst Eng Mater 72(Pt 2) (2016) 171-9.
[37] I.R. Thomas, I.J. Bruno, J.C. Cole, C.F. Macrae, E. Pidcock, P.A. Wood, WebCSD: the online portal to the Cambridge Structural Database, J. Appl. Crystallogr. 43 (2010) 362-366.
[38] J.A. Maddry, B.S. Joshi, A.A. Ali, M.G. Newton, S.W. Pelletier, REVISED STRUCTURES OF PRATORININE AND PRATORIMINE, Tetrahedron Letters 26(36) (1985) 4301-4302.
[39] H.S. Kim, M.G. Banwell, A.C. Willis, Convergent total syntheses of the Amaryllidaceae alkaloids lycoranine A, lycoranine B, and 2-methoxypratosine, J Org Chem 78(10) (2013) 5103-9.
[40] A.I. Kitajgorodskij, Molecular Crystals and Molecules, Academic Press, New York, 1973.
[41] A.J.C. Wilson, V.L. Karen, A. Mighell, The space-group distribution of molecular organic structures, in: E. Prince (Ed.), International Tables for Crystallography Volume C: Mathematical, physical and chemical tables, Springer Netherlands, Dordrecht, 2004, pp. 897-906.
[42] P. Kraft, A. Bergamaschi, C. Broennimann, R. Dinapoli, E.F. Eikenberry, B. Henrich, I. Johnson, A. Mozzanica, C.M. Schleputz, P.R. Willmott, B. Schmitt, Performance of single-photon-counting PILATUS detector modules, J. Synchrot. Radiat. 16 (2009) 368-375.
[43] A. Burkhardt, T. Pakendorf, B. Reime, J. Meyer, P. Fischer, N. Stube, S. Panneerselvam, O. Lorbeer, K. Stachnik, M. Warmer, P. Rodig, D. Gories, A. Meents, Status of the crystallography beamlines at PETRA III, Eur. Phys. J. Plus 131(3) (2016) 1-9.
[44] W. Kabsch, XDS, Acta Crystallogr. Sect. D-Biol. Crystallogr. 66 (2010) 125-132.
[45] G.M. Sheldrick, SHELXT - integrated space-group and crystal-structure determination, Acta Crystallogr A Found Adv 71(Pt 1) (2015) 3-8.
[46] G.M. Sheldrick, Crystal structure refinement with SHELXL, Acta Crystallogr C Struct Chem 71(Pt 1) (2015) 3-8.
[47] K. Brandenburg, DIAMOND, Crystal Impact GbR, Bonn, Germany, 2016.